Magnetic susceptibility and electrical resistivity of dilute liquid copper - iron alloys

1996 J. Phys.: Condens. Matter 8 7041

(http://iopscience.iop.org/0953-8984/8/38/008)

J. Phys.: Condens. Matter **8** (1996) 7041–7048. Printed in the UK

Magnetic susceptibility and electrical resistivity of dilute liquid copper–iron alloys

P Terzieff† and J G Gasser‡

† Institut für Anorganische Chemie, Universität Wien, Währingerstraße 42, A-1090 Wien, Austria
‡ Laboratoire de Physique des Liquides et des Interfaces, Université de Metz, 1 Boulevard Arago, 57070 Metz, France

Received 21 March 1996

Abstract. Electrical resistivity and magnetic susceptibility measurements on dilute liquid **Cu**Fe alloys are reported. Small additions of Fe increase the resistivity of liquid Cu in a drastic manner, whereas the temperature coefficient is found to be decreased. Due to the localized magnetic moments of the impurity atoms the diamagnetism of Cu is converted into a strong temperature-dependent paramagnetism indicating about 3.5 unpaired d electrons per Fe atom. The electronic properties of **Cu**Fe resemble those of liquid **Cu**Mn and **Au**Fe which, in the solid state, are known for their Kondo-like behaviour. The experimental findings are tentatively interpreted in terms of spin-disorder scattering with special emphasis on the negative temperature coefficient of the impurity resistivity.

1. Introduction

In the past, much attention has been paid to the transport properties in liquid alloys of first-row transition elements with normal metals. In general, many of the characteristic trends are well understood in terms of the rigid-band model or the theory of Faber and Ziman [1]. According to the valency of the added metal, two categories of alloy can be distinguished: alloying with polyvalent metals increases the abundance of conduction electrons which may result in (i) a filling-up of the transition metal d band and (ii) a systematic shift of the Fermi vector k_F to values beyond the first maxima of the partial structure factors. As a consequence, the magnetic moments tend to disappear in a gradual manner while—at certain concentrations—the electrical resistivities pass through characteristic maxima associated with negative temperature coefficients. Alloying of transition metals with monovalent metals like Cu, Ag or Au, on the other hand, hardly affects the occupancy of the d bands and the value of k_F which yields a normal electronic behaviour.

Although these empirical rules have proved to be useful for a first understanding, particularly if non-transition elements are involved [2], the classification of transition metal alloy systems into one of these two categories seems to be problematic. In liquid Fe–Sn the magnetic moments decrease due to the addition of tetravalent Sn, but they never disappear [3]; alloys of Mn with monovalent Cu exhibit electrical resistivities with definitely negative temperature coefficients [2]. A recent investigation of the electrical resistivity in liquid Au–Fe yielded similar results indicating that the exceptional behaviour of Cu–Mn is not unique but rather common to all systems with highly localized magnetic moments [4]. It is unclear how far the unexpected electronic behaviour of Cu–Mn or Au–Fe can be assigned to spin-disorder scattering, i.e. to the interaction between the localized spins and the conduction

0953-8984/96/387041+08$19.50

electrons. In view of this important but still open question it seemed to be of special interest to investigate the electronic behaviour of the homologous system Cu–Fe.

2. Experimental details

High-purity copper slugs (99.999%, Johnson–Matthey) and iron wire (99.98%, Johnson–Matthey) were used as starting materials. Prior to the magnetic measurements the samples (≈0.6 g) were brought into homogeneous liquid form by a suitable thermal treatment (24 h at 1400 K, in evacuated quartz ampoules). The measurements were performed under a protective argon atmosphere on a Faraday-type balance working at a magnetic field strength of 19 kOe. The temperature was changed at a rate of about 5 K min^{-1}, and data points were recorded at a variable rate of 2–5 points min^{-1}.

A capillary method was applied to determine the electrical resistivities. The measurements were performed in a quartz cell under an argon pressure of about 2 bar using a quartz capillary equipped with four tungsten electrodes; the calibration refers to the room temperature resistivity of high-purity mercury (95.783 $\mu\Omega$ cm).

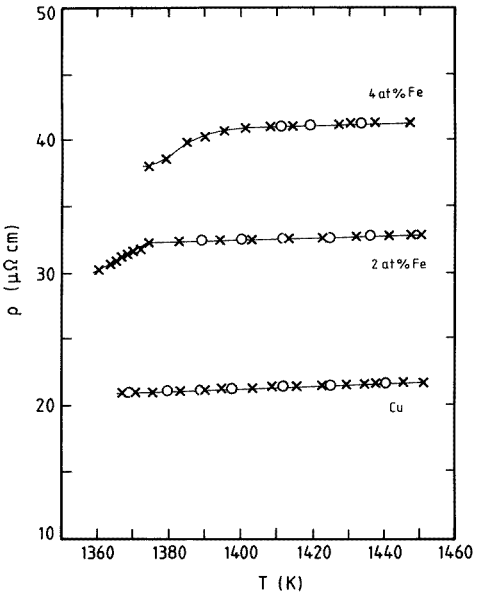

Figure 1. The temperature dependence of the electrical resistivity in liquid Cu and dilute **Cu**Fe alloys (○: heating; ×: cooling).

Starting with pure elemental copper, the composition of the melt was changed *in situ* by adding appropriate amounts of iron. The completeness of the equilibration process was verified by continually controlling the changes in the electrical resistivity. The experimental accuracy of the reported electrical resistivities was about 1%; that of the magnetic susceptibility was better than 3%.

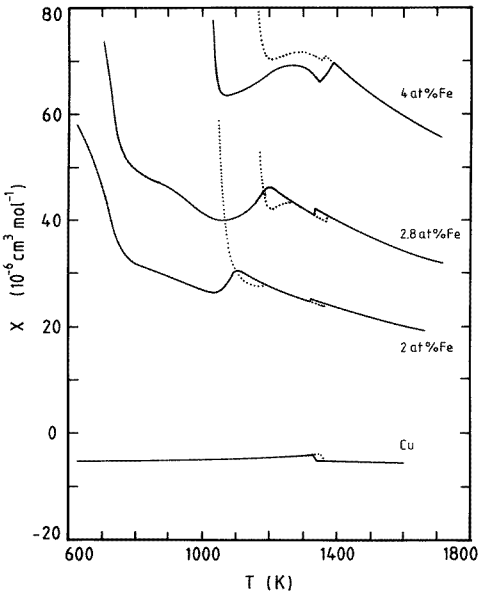

Figure 2. The temperature dependence of the magnetic susceptibility in the liquid and solid states of Cu and dilute **Cu**Fe alloys (· · ·, heating; ——, cooling).

3. Experimental results

Due to experimental limitations with respect to temperature only a small portion of the phase diagram was accessible to our measurements. Up to about 4 at.% Fe the liquidus temperatures are not much higher than that of pure Cu (1358 K); however, the further addition of Fe leads to a dramatic increase of the liquidus temperature [5]. Therefore, this study was focused on pure liquid Cu, and the dilute alloys $Cu_{98}Fe_{02}$ and $Cu_{96}Fe_{04}$.

The electrical resistivity of Cu was found to be extremely sensitive to the presence of Fe impurities (figure 1). The addition of 2 and 4 at.% Fe increases the resistivity by 50 and 100%, respectively. The variation with the temperature is linear in the range of the homogeneous liquid, the anomalies on the low-temperature side reflect the solidification process which is expected to occur more abruptly in $Cu_{98}Fe_{02}$, and rather smoothly in $Cu_{96}Fe_{04}$, in accordance with the phase diagram [5].

Table 1. Magnetic data and Friedel–Anderson model parameters of liquid **Cu**Fe calculated for a half-width of $\Gamma/2 = 0.4$ eV and an exchange energy of $U_{ex} = 7$ eV: magnetic moment (μ_{eff}), impurity spin (S), paramagnetic Curie temperature (θ), position of the virtual bound states ($E_\uparrow - E_F$, $E_\downarrow - E_F$), and d-wave phase shifts ($\eta_\uparrow$, $\eta_\downarrow$).

Composition (at.% Fe)	μ_{eff} (μ_B)	S	θ (K)	$E_\uparrow - E_F$ (eV)	$E_\downarrow - E_F$ (eV)	$\eta_\uparrow$	$\eta_\downarrow$
0	(diamagnetic)		—	—	—	—	—
2.0	4.35	1.73	256	−2.01	0.42	2.95	0.77
2.8†	4.43	1.77	132	—	—	—	—
4.0	4.66	1.88	76	−2.01	0.63	2.95	0.58

†Ill-defined composition of 2.8 ± 0.5 at.% Fe.

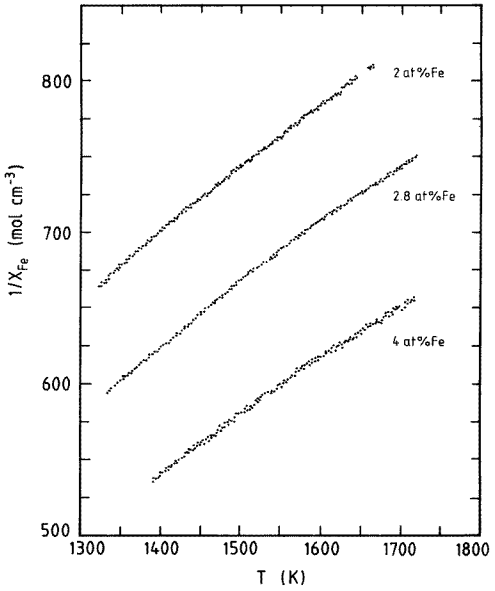

Figure 3. The temperature dependence of the inverse impurity susceptibility in liquid dilute **Cu**Fe.

The results of the magnetic measurements are shown in figure 2 which also includes an alloy with the approximate composition of 2.8 ± 0.5 at.% Fe. It is apparent that small amounts of Fe superimpose a strong temperature-dependent component onto the diamagnetic susceptibility of liquid Cu due to the magnetic moments of the Fe atoms. Consequently, the total magnetic susceptibility was considered to be the sum of the diamagnetic contribution of the host metal and a paramagnetic term originating from the impurity atoms according to

$$\chi_{tot} = x_{Cu}\chi_{Cu} + x_{Fe}\chi_{Fe}. \tag{1}$$

The variation of $1/\chi_{Fe}$ with the temperature (illustrated in figure 3) implies that χ_{Fe} follows a Curie–Weiss-like behaviour expressed in terms of the Curie constant C and the paramagnetic Curie temperature θ:

$$\chi_{Fe} = C/(T + \theta). \tag{2}$$

The effective magnetic moments μ_{eff} were deduced from the Curie constant C via the classical relation

$$\mu_{eff} = 2.83\sqrt{C} \tag{3}$$

which yields 4.35 μ_B per Fe atom in $Cu_{98}Fe_{02}$, and 4.66 μ_B in $Cu_{96}Fe_{04}$. This is in excellent agreement with the value 4.53 μ_B quoted for liquid **Cu**Fe by Gardner and Flynn [6], and also with the values reported by Nakagawa [7] for concentrated alloys of CuFe, but considerably smaller than the value 5.14 μ_B observed by Gruber and Gardner in their study on ternary liquid **CuAl**Fe [8].

The numerical results are listed in table 1 together with some model parameters. The small deviation from a strict linearity between $1/\chi_{Fe}$ and T in figure 3 is probably due to the assumed additivity of the magnetic susceptibilities as expressed by equation (1). This paper is not aimed at investigating the magnetic properties of solid-state **Cu**Fe, but it is obvious that the anomalies observed on cooling are associated with the solidification reaction, followed by the precipitation of fcc Fe, and finally with the transition into the magnetically ordered state

Table 2. Electrical resistivity of liquid **Cu**Fe at 1420 K: x, experimental values; a, resonance scattering resistivity calculated in simple form; b, with split phase shifts; b′, in the dilute-case approximation; c, spin-disorder resistivity uncorrected; d, corrected for simple resonance scattering; e, corrected with split phase shifts.

Composition (at.% Fe)	Electrical resistivity ($\mu\Omega$ cm)						
	x	a	b	b′	c	d	e
0	21.49	28.50	28.50	21.49	0	0	0
2.0	32.68	31.74	32.24	34.82	11.19	7.96	7.46
4.0	41.18	34.91	32.86	40.68	19.69	13.29	14.34

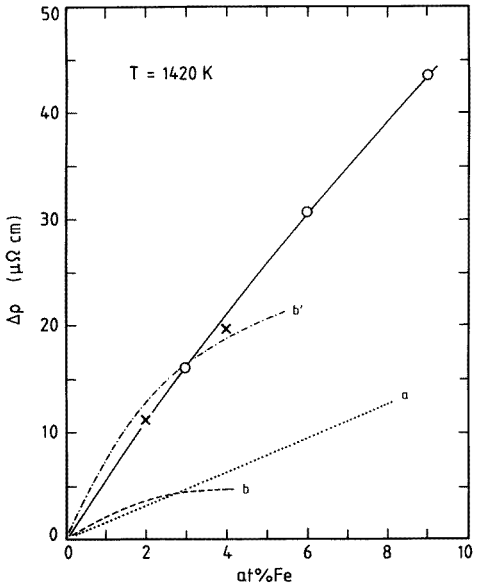

Figure 4. The composition dependence of the residual resistivity in liquid **Cu**Fe at 1420 K: ×, experimental values; a, the resonance scattering approach in simple form; b, with split phase shifts; b′, in the dilute-case approximation; ○, experimental data for **Au**Fe [4].

Table 3. The temperature coefficient of the electrical resistivity of liquid **Cu**Fe: x, experimental values; a, resonance scattering contribution calculated in simple form; b, with split phase shifts; c, spin-disorder scattering contribution uncorrected; d, corrected for simple resonance scattering; e, corrected with split phase shifts.

Composition (at.% Fe)	$d\rho/dT$ (nΩ cm^{-1} K^{-1})					
	x	a	b	c	d	e
0	8.61	9.80	9.80	0	0	0
2.0	6.61	10.22	10.04	−4.95	−2.96	−2.69
4.0	6.77	10.68	10.18	−7.61	−4.22	−5.23

(figure 2). The divergencies observed between heating and cooling on the low-temperature

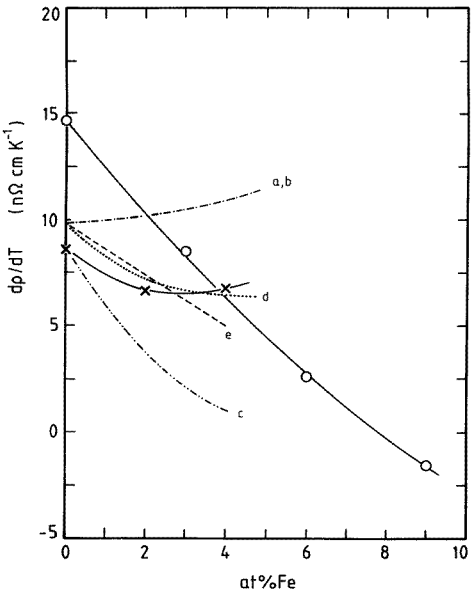

Figure 5. The temperature coefficient of the electrical resistivity in liquid Cu and dilute **Cu**Fe: ×, experimental values; a, the resonance scattering contribution in simple form; b, with split phase shifts; c, spin-disorder scattering approach uncorrected; d, corrected for simple resonance scattering; e, corrected with split phase shifts; ○, experimental data for **Au**Fe [4].

side are the result of uncompleted phase reactions due to finite heating and cooling rates.

4. Discussion

A more elaborate analysis of the experimental results in terms of the Faber–Ziman theory reveals a strong similarity to the liquid system **Au**Fe which has been discussed in much detail in a previous article [4]. The residual resistivities (the resistivity increments due to the impurities, $\Delta\rho = \rho - \rho_{Cu}$) increase in the same drastic manner (figure 4) and the temperature coefficients—although this is less pronounced in **Cu**Fe than in **Au**Fe—decrease with increasing content of Fe (figure 5). The theoretical predictions obtained from the resonance scattering formulation of the Faber–Ziman theory [9] by using the phase shifts proposed by Waseda [10] are obviously incompatible with the experimental findings (curve a in figure 4 and figure 5, column a in table 2 and table 3). This, on the other hand, is not surprising since the treatment of resonance scattering in terms of a magnetically unsplit band structure does not take account of the magnetic moments associated with the Fe atoms. The marked discrepancies, most evident in the temperature coefficients, have tempted us to assume that spin-disorder scattering, i.e. the s–d interaction between conduction electrons and impurity spin, might be responsible for the unexpected behaviour of the systems under discussion. If, in a first approximation, the residual resistivities are assigned entirely to spin-disorder scattering ($\Delta\rho = \rho_{spin}$), the s–d interaction energy J_{eff} can be deduced from the relation proposed by Kondo [11]

$$\rho_{spin} = \frac{3\pi m_e}{2he^2}\frac{\Omega}{E_F}x_{Fe}S(S+1)J_{eff}^2. \tag{4}$$

The temperature coefficient, on the other hand, can be derived from the expression

$$T\ \frac{\mathrm{d}\rho_{spin}}{\mathrm{d}T} = 3z\rho_{spin}\frac{J_{eff}}{E_F}. \tag{5}$$

E_F denotes the Fermi energy, m_e the electron mass, Ω the atomic volume, z the formal valency of the host metal, and S the spin per impurity atom. With the values of S deduced from μ_{eff} via the relation

$$\mu_{eff} = 2\sqrt{S(S+1)}\mu_B \tag{6}$$

equation (4) yields $J_{eff} = -1.69$ eV for the alloy with 2 at.% Fe and $J_{eff} = -1.48$ eV for that with 4 at.% Fe. Due to the exclusion of other contributions to the residual resistivity (e.g. the structural contribution according to Faber and Ziman [1] represented by the resonance scattering approach), these values are presumably only the lower limit of J_{eff}; as a result, the experimental trend of the temperature coefficient is only roughly reproduced (curve c in figure 5, column c in table 2 and table 3).

Assuming that both spin-disorder scattering and resonance scattering contribute to the residual resistivity, i.e. $\Delta\rho = \rho_{res} + \rho_{spin}$, we arrive at $J_{eff} = -1.42$ eV (2 at.% Fe) and $J_{eff} = -1.21$ eV (4 at.% Fe) which are comparable to the value found for liquid **Au**Fe ($J_{eff} \approx -1.3$ eV) [4]. This gives already a very good description of the experimental temperature coefficients (curve d in figure 5, column d in table 2 and table 3); however, it has to be emphasized that the Faber–Ziman formula was evaluated with unsplit phase shifts. It has been shown for liquid **Au**Fe how the Faber–Ziman formula can be adapted so as to be in accordance with the magnetic properties of the system [4]. An adequate set of split phase shifts can be deduced from the model put forward by Friedel [12] and Anderson [13]. By analogy to liquid **Au**Fe, the half-width of virtual d bands $\Gamma/2$ was assumed to be 0.4 eV, and the splitting of the spin-up and spin-down band $E_\uparrow - E_\downarrow$ was based on an exchange energy $U_{ex} \approx 7$ eV which, together with our experimental values of S, permitted us to calculate the spin-up part $\eta_\uparrow$ and the spin-down part $\eta_\downarrow$ of the d-wave phase shift according to

$$\eta_\uparrow = \tan^{-1}\left[\frac{\Gamma/2}{E_\uparrow - E_F}\right] \qquad \eta_\downarrow = \tan^{-1}\left[\frac{\Gamma/2}{E_\downarrow - E_F}\right] \tag{7}$$

and the additional conditions

$$\eta_\uparrow - \eta_\downarrow = \frac{2}{5}\pi S \qquad \text{and} \qquad E_\uparrow - E_\downarrow = \frac{2}{5}SU_{ex}. \tag{8}$$

The results are summarized in table 1. Our analysis yielded a nearly filled majority band (93%) located about 2 eV below E_F, and a moderately filled minority band (22%) located 0.5 eV above E_F. The treatment of Pantasis and Wachtel performed for liquid **CuAl**Fe [14] led to subbands located 4.2 eV below E_F (98%), and 0.7 eV above E_F (17%), respectively, with half-widths of 0.4 eV. In this context it is worth noting that theoretical calculations for solid **Cu**Fe [15] suggest a very narrow filled majority band ($\Gamma/2 \approx 0.1$ eV) located at 1.5 eV below E_F, and a broad half-filled minority band ($\Gamma/2 \approx 1$ eV) around E_F, whereas experimental XPS studies failed to give any evidence of well defined virtual bound-impurity states [16].

As regards the interpretation of our resistivity data the improvements brought about by introducing such a set of split phase shifts into the Faber–Ziman formula are not essential. The calculated residual resistivities are still smaller by a factor of 3 than the experimental values (curve b in figure 4, column b in table 2), and the temperature coefficients increase with the impurity concentration, in contrast to the experimental trend

(curve b in figure 5, column b in table 3). Even the combination with a spin-scattering contribution ($\Delta\rho = \rho_{res} + \rho_{spin}$) fails to improve the description of the experimental findings (curve e in figure 5, column e in table 3).

Judged by the variation of the residual resistivity itself, the approximation for the dilute case (i.e. for small impurity concentrations, c) would have given a correct answer. In fact, using the expression

$$\Delta\rho = \frac{5hc}{ze^2k_F}(\sin^2\eta_\uparrow + \sin^2\eta_\downarrow) \tag{9}$$

and assuming the majority band to be completely filled (i.e. $n_\uparrow \approx 5$, or $\eta_\uparrow \approx \pi$) and the occupancy of the minority band to be related to the spin number S (i.e. $n_\downarrow \approx 2S$, or $\eta_\downarrow \approx 2\pi S/5$) the experimental curve turns out to be well reproduced (curve b′ in figure 4, column b′ in table 2). However, such a crude approximation implies a negligibly small positive temperature coefficient (via the Fermi vector k_F) instead of the observed negative temperature coefficient of the residual resistivity.

Despite the successful interpretation of the extraordinary properties of liquid **Au**Fe via the concept outlined above, its application to liquid **Cu**Fe seems to be crudely justified. The initial idea of this paper was to analyse those liquid systems which exhibit a Kondo-like behaviour in the solid state in a systematic manner. Although there is no real need for taking spin-disorder scattering into consideration, it seems that the Kondo systems **Cu**Mn, **Au**Fe and **Cu**Fe share many common features which are presumably related to the localized magnetic moments of the transition metal impurities.

References

[1] Faber T E and Ziman J M 1965 *Phil. Mag.* **11** 153
[2] Güntherodt H J and Künzi H U 1973 *Phys. Kondens. Mater.* **16** 117
[3] Terzieff P and Lück R 1994 *J. Alloys Compounds* **203** 139
[4] Terzieff P and Gasser J G 1994 *J. Phys.: Condens. Matter* **6** 603
[5] Moffat W G 1984 *The Handbook of Binary Phase Diagrams* (New York: Genium)
[6] Gardner J A and Flynn C P 1967 *Phil. Mag.* **15** 1233
[7] Nakagawa J 1959 *J. Phys. Soc. Japan* **14** 1372
[8] Gruber O F and Gardner J A 1971 *Phys. Rev.* B **4** 3994
[9] Evans R, Greenwood D A and Lloyd P 1971 *Phys. Lett.* **35A** 57
[10] Waseda Y 1980 *The Structure of Non-Crystalline Materials* (New York: McGraw-Hill)
[11] Kondo J 1964 *Prog. Theor. Phys.* **33** 559
[12] Friedel J 1962 *J. Physique Radium* **23** 692
[13] Anderson P W 1961 *Phys. Rev* **124** 41
[14] Pantasis A and Wachtel E 1978 *J. Magn. Magn. Mater.* **9** 264
[15] Zeller R, Podloucky R and Dederichs P H 1980 *Z. Phys.* B **38** 165
[16] Höchst H, Steiner P and Hüfner S 1980 *Z. Phys.* B **38** 201